

# Effect of $Y_2O_3$ on low temperature sintering and thermal conductivity of AlN ceramics

Liang Qiao\*, Heping Zhou, Hao Xue, Shaohong Wang

*Skate Key Laboratory of New Ceramics and Fine Processing, Department of Materials Science and Engineering, Tsinghua University, Beijing, 100084, People's Republic of China*

Received 26 October 2001; received in revised form 21 February 2002; accepted 11 March 2002

## Abstract

The effect of  $Y_2O_3$  on the densification and thermal conductivity of AlN ceramics sintered at the temperature of 1650 °C was studied using  $CaF_2$ – $Y_2O_3$  system as additives. XRD was employed to identify the phases formed during sintering. The results show that AlN ceramics with  $Y_2O_3$  addition have a low shrinkage at temperatures below 1600 °C because the solid reaction between  $Y_2O_3$  and  $Al_2O_3$  decreases the amount of the calcium aluminates liquid due to the consumption of  $Al_2O_3$ . At 1650 °C,  $Y_2O_3$  promotes the densification due to the formation of liquid  $CaYAlO_4$ . The observation by TEM and HREM reveals that the inhomogeneous grain-boundary phases containing different phase compositions move to the three-grain junctions to form discrete pockets during the sintering. The measurement of the lattice parameters and the thermal conductivity of AlN ceramics shows that  $Y_2O_3$  has no prominent effect on the purification of the AlN lattice at this sintering temperature. The higher thermal conductivity in the presence of  $Y_2O_3$  mainly comes from the enhancement of the densification. © 2002 Elsevier Science Ltd. All rights reserved.

*Keywords:* AlN; Grain boundary phases; Sintering; Thermal conductivity

## 1. Introduction

Aluminum nitride is considered to be a promising substrate and package material for high power integrated circuits because of its high thermal conductivity, low dielectric constant, thermal expansion coefficient close to that of silicon and high electrical resistivity.<sup>1–3</sup> However, AlN is difficult to sinter due to its highly covalent bonding. For full densification, rare-earth and/or alkaline earth oxides are often added as sintering aids in the fabrication of AlN ceramics.<sup>4,5</sup> These sintering aids play a double role during the sintering. One is to help form the liquid phase that promotes the densification by the process of liquid-phase sintering. The other is to improve the thermal conductivity by decreasing the oxygen impurities in the AlN lattice.  $Y_2O_3$  is an effective additive to achieve dense AlN ceramics most likely due to the liquid-phase formation of yttrium aluminates at temperatures around 1800 °C since the eutectic temperature of  $Y_2O_3$  and  $Al_2O_3$  is around this region.<sup>6</sup>

Also, it purifies the AlN lattice by forming YAP and YAM with low activity of  $Al_2O_3$  in them, which increases the thermodynamic driving force for oxygen removal, and thus increases the thermal conductivity of AlN ceramics.<sup>7,8</sup> Recently more and more attention has been given on the low temperature sintering of AlN ceramics considering reducing manufacturing cost and benefiting cofiring of multilayer substrates.<sup>9–15</sup> In these studies,  $Y_2O_3$  is often used as one of the additives.<sup>9,11,12,13</sup> However, its effect on the densification and thermal conductivity is not clear enough. Jarrige et al.<sup>12</sup> found that  $Y_2O_3$  increases the viscosity of the calcium aluminates and limits the composition change of the liquid to refractory phases by displacing the composition of the secondary phases at 1700 °C. However, they did not give the effect of  $Y_2O_3$  on the thermal conductivity of the sintered specimens. At the temperature lower than 1700 °C, whether  $Y_2O_3$  has an important role on the elimination of oxygen defects in the AlN lattice is also unknown. In this paper,  $CaF_2$  and  $Y_2O_3$  were used as additives to study the effect of  $Y_2O_3$  on the densification and thermal conductivity of AlN ceramics at the temperature of 1650 °C.

\* Corresponding author.

*E-mail address:* [qiaoliang98@mails.tsinghua.edu.cn](mailto:qiaoliang98@mails.tsinghua.edu.cn) (L. Qiao).

## 2. Experimental

Specimens were prepared through a conventional ceramic fabrication process. Commercially available AlN powder (grade US, Toyo Aluminium K. K.), as described by Table 1, was used as a starting material. Powders of AlN with additives of CaF<sub>2</sub> (analytical reagents) and Y<sub>2</sub>O<sub>3</sub> (analytical reagents) were ball-milled by planetary milling for 2 h using ethanol as a mixing medium. After drying and binder-adding, the powder mixture was uniaxially die-pressed into pellets 10 mm in diameter and 5 mm thick and then de-waxed at 550 °C. The pellets were then placed into a BN crucible and sintered at 1650 °C for 1 min, 2 h, 4 h, 6 h and 12 h respectively in a graphite furnace with a flowing nitrogen atmosphere. The compositions of the specimens were shown in Table 2.

The shrinkages and the densities of the sintered pellets were measured by vernier caliper and Archimedes displacement method, respectively. X-ray diffraction (XRD) with CuK<sub>α</sub> was used to identify the produced phases. The fracture surfaces of the pellets were observed by scanning electron microscopy (SEM, OPTON, CSM950). The liquid phases between the grains were examined by transmission electron microscopy (JEM, 200CX) and high resolution transmission electron microscopy (JEM, 2010F). To determine the lattice parameters, the samples with and without Y<sub>2</sub>O<sub>3</sub> addition fired for 1 min, 4 h and 8 h at 1650 °C were scanned from 90 to 140° at the rate of 0.1°/min using CuK<sub>α</sub> radiation. The thermal conductivity at room temperature was measured by a laser flash technique.

To identify the phases in the sintering, Al<sub>2</sub>O<sub>3</sub> was added in the additives as one of the reactants, as described by Table 2. Then the mixed powders fired at 1200 °C were identified by XRD. As the liquid may

occur at a higher temperature, the mixed powders, laid on the single AlN pellets, were fired at 1650 °C in a graphite furnace with a flowing nitrogen atmosphere, just like the sintering of AlN ceramics. After being fired for different times, the AlN pellets penetrated by the liquid were identified by XRD to achieve the phase compositions in the liquid.

## 3. Results

### 3.1. Shrinkage

Fig. 1 shows the shrinkage of the samples with different amounts of Y<sub>2</sub>O<sub>3</sub> addition. Compared with sample CA, the samples with Y<sub>2</sub>O<sub>3</sub> addition have lower shrinkages at temperatures lower than 1600 °C. However, the shrinkages of samples CYA1 and CYA2 increase quickly and exceed that of sample CA above 1600 °C. After sintered at 1650 °C for 12 h, sample CYA1 shrinks 17.9%, higher than that of the sample without Y<sub>2</sub>O<sub>3</sub> addition, which is 16.3%. It also can be seen in the figure that sample CYA1 has the largest shrinkages in the three samples with Y<sub>2</sub>O<sub>3</sub> addition, which indicates that 2 wt.% Y<sub>2</sub>O<sub>3</sub> benefits achieving a maximum of shrinkages. The different shrinkages of the samples with Y<sub>2</sub>O<sub>3</sub> addition are most likely attributed to the effects of Y<sub>2</sub>O<sub>3</sub> on the liquid phases during the different sintering temperatures, as the following explains in detail.

### 3.2. Phase compositions

The phases in the sintered samples CAO and CYAO were summarized in Table 3. At 1200 °C, CaF<sub>2</sub> reacts with Al<sub>2</sub>O<sub>3</sub> to form CaAl<sub>4</sub>O<sub>7</sub>, CaAl<sub>2</sub>O<sub>4</sub> and Ca<sub>12</sub>Al<sub>14</sub>F<sub>2</sub>O<sub>32</sub>. When Y<sub>2</sub>O<sub>3</sub> is added with CaF<sub>2</sub>, the additional phases Y<sub>4</sub>Al<sub>2</sub>O<sub>9</sub> (YAM) and CaYAl<sub>3</sub>O<sub>7</sub> are identified. Since both Ca–Al–O compounds and yttrium aluminates are formed at this temperature, the amount of Y<sub>2</sub>O<sub>3</sub> influences the formation of Ca–Al–O compounds due to the

Table 1  
Properties of the starting AlN powder

Chemical composition (wt.%)					Average particle size (μm)	Specific surface (m <sup>2</sup> g <sup>-1</sup> )
N	O	C	Si	Fe		
33.2	1.11	0.04	0.0059	0.0023	1.46	4.50

Table 2  
Compositions of different samples in the experiments

Sample	CaF <sub>2</sub> (wt.%)	Y <sub>2</sub> O <sub>3</sub> (wt.%)	Al <sub>2</sub> O <sub>3</sub> (wt.%)	AlN (wt.%)
CA	2	0	0	98
YA	0	2	0	98
CYA1	2	2	0	96
CYA2	2	3.5	0	94.5
CAO	44.4	0	55.6	0
YAO	0	44.4	55.6	0
CYAO	30.8	30.8	38.4	0

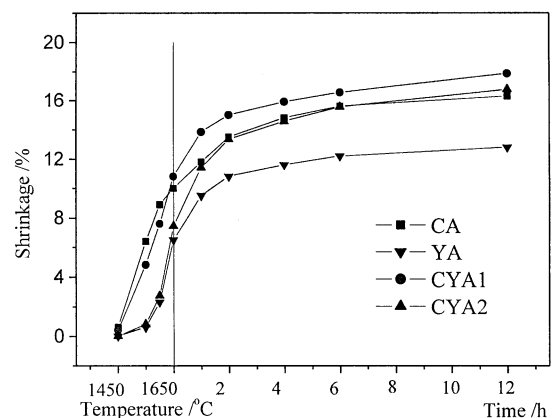


Fig. 1. The shrinkage of samples during the firing.

consumption of  $\text{Al}_2\text{O}_3$ . Thus, when sintered at temperatures lower than  $1650^\circ\text{C}$ , the lower shrinkage in the samples with  $\text{Y}_2\text{O}_3$  addition may be attributed to the decreased amount of the calcium aluminates liquid, which generally promotes the densification of AlN ceramics. At  $1650^\circ\text{C}$ , a trace of  $\text{CaAl}_4\text{O}_7$  remains in sample CAO, while in sample CYAO,  $\text{CaYAlO}_4$  is an additional phase besides the calcium aluminates and YAM. After being sintered for 8 h, Ca–Al–O compounds except for a trace of  $\text{CaAl}_2\text{O}_4$  are nearly undetectable in sample CAO, which implies evaporation of the Ca–Al–O compounds in a carbon-containing nitrogen atmosphere, as mentioned by Greil.<sup>16</sup> But in sample CYAO sintered for 8 h, the compounds containing CaO– $\text{Y}_2\text{O}_3$ – $\text{Al}_2\text{O}_3$  still exist, which implies that these phases are stable at this temperature. Since the quick shrinkages of the samples with  $\text{Y}_2\text{O}_3$  addition and phase  $\text{CaYAlO}_4$  occur near  $1650^\circ\text{C}$ , it is possible that the liquid phases containing  $\text{CaYAlO}_4$  promote the densification of AlN ceramics during sintering at  $1650^\circ\text{C}$ .

Using XRF, the contents of elements Ca and Y are detected in the polished sample CYA1 sintered for different times at  $1650^\circ\text{C}$ . As shown in Fig. 2, Ca content decreases with the soaking time, which associates with the evaporation of calcium aluminates. After being sintered for 6 h, the decrease of Ca content becomes slow, which implies that  $\text{CaYAlO}_4$  is stably remaining in the sample. Y content has a different change from Ca content in that it decreases quickly after being sintered for 6 h. This may come from the removal of the liquid containing the yttrium aluminates from the interior to the surface of the specimens during the sintering.

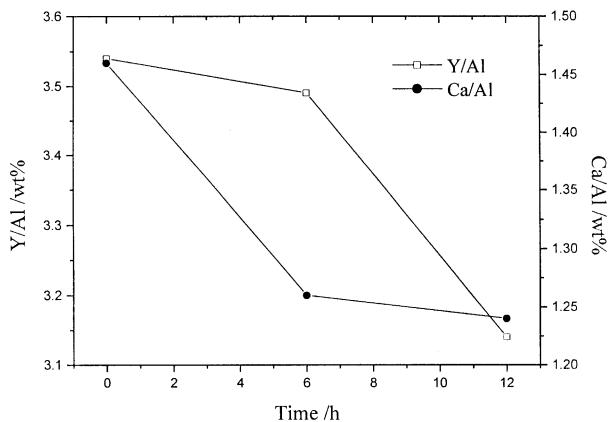


Fig. 2. Y and Ca contents in the sample CYA1 sintered at  $1650^\circ\text{C}$  for different time.

Table 3  
Phase compositions of different samples during the firing

	CAO	CYAO
1200 °C for 1 h	$\text{CaF}_2$ , $\text{Al}_2\text{O}_3$ , $\text{CaAl}_2\text{O}_4$ , $\text{CaAl}_4\text{O}_7$ , $\text{Ca}_{12}\text{Al}_{14}\text{F}_2\text{O}_{32}$	$\text{CaF}_2$ , $\text{Ca}_{12}\text{Al}_{14}\text{F}_2\text{O}_{32}$ , $\text{Y}_4\text{Al}_2\text{O}_9$ , $\text{YAlO}_3$ , $\text{CaYAl}_3\text{O}_7$
1650 °C for 1 min	$\text{CaAl}_2\text{O}_4$	$\text{Y}_4\text{Al}_2\text{O}_9$ , $\text{Y}_3\text{Al}_5\text{O}_{12}$ , $\text{Ca}_2\text{Al}_2\text{O}_5$ , $\text{CaYAl}_3\text{O}_7$ , $\text{CaYAlO}_4$
1650 °C for 8 h	Trace of $\text{CaAl}_2\text{O}_4$	$\text{Y}_4\text{Al}_2\text{O}_9$ , $\text{CaYAl}_3\text{O}_7$ , $\text{CaYAlO}_4$

### 3.3. Microstructure

Figs. 3 and 4 show the microstructure of the fracture surface of samples CA and CYA1 sintered at  $1650^\circ\text{C}$  for 1 min, 6 h and 12 h, respectively. From the photographs, it is observed that a large quantity of liquid congregates together in the samples sintered for 1 min but is homogeneously distributed between the grains after 6 h. This shows that the liquid goes through a process from occurrence to redistribution during the sintering. In sample CA the grains have an inhomogeneous size distribution. However, they are more homogeneous in sample CYA1, which implies that  $\text{CaYAlO}_4$  improves the growth of the AlN grains. Furthermore, the fracture is along the grains in sample CA sintered for 12 h, but in sample CYA1, it is visible that fracture surfaces across some grains, as shown in Fig. 4(c). This implies that the bonding between the AlN grains can be enhanced in the presence of  $\text{Y}_2\text{O}_3$ .

As shown in Fig. 5, the dihedral angles between the grains of both sample CA and CYA1 sintered for 4 h are close to  $120^\circ$ , which implies the grain-boundary phases have a less wetting to the AlN grains. This agrees with the high viscosity of the secondary phases as Jarrige et al. mentioned.<sup>12</sup> The less wetting also results in the less final shrinkages of samples CA and CYA1 compared with the results achieved by Wang et al.<sup>17</sup> In sample without  $\text{Y}_2\text{O}_3$  addition, the amount of the grain-boundary phases is so small that the clean grain boundaries remain due to the evaporation of the grain-boundary phases, as shown in Fig. 5(a). In the sample with  $\text{Y}_2\text{O}_3$ , a few of grain-boundary phases move to the three-grain junctions, thus also resulting in the sharp grain boundaries, as shown in Fig. 5(b).

The high resolution TEM picture of the grain-boundary phases in sample CYA1 sintered for 4 h is shown in Fig. 6. Two fields with different atom arrangements are observed from the figure. The interlayer spacings along the orthogonal directions in the field I are 1.038 and 1.045 nm, approximately equal to the plane spacings of (010) and (100) of phase YAM, which are 1.0469 and 1.0528 nm, respectively. The selected area electron diffractive pattern at this area also indicates the existence of YAM phase as shown in this figure. In the field II, the interlayer spacings along the two perpendicular directions are 0.379 and 1.163 nm, in agreement with the plane spacings of (100) and (010) of  $\text{CaYAlO}_4$  phase, which are 0.364 and 1.187 nm, respectively.

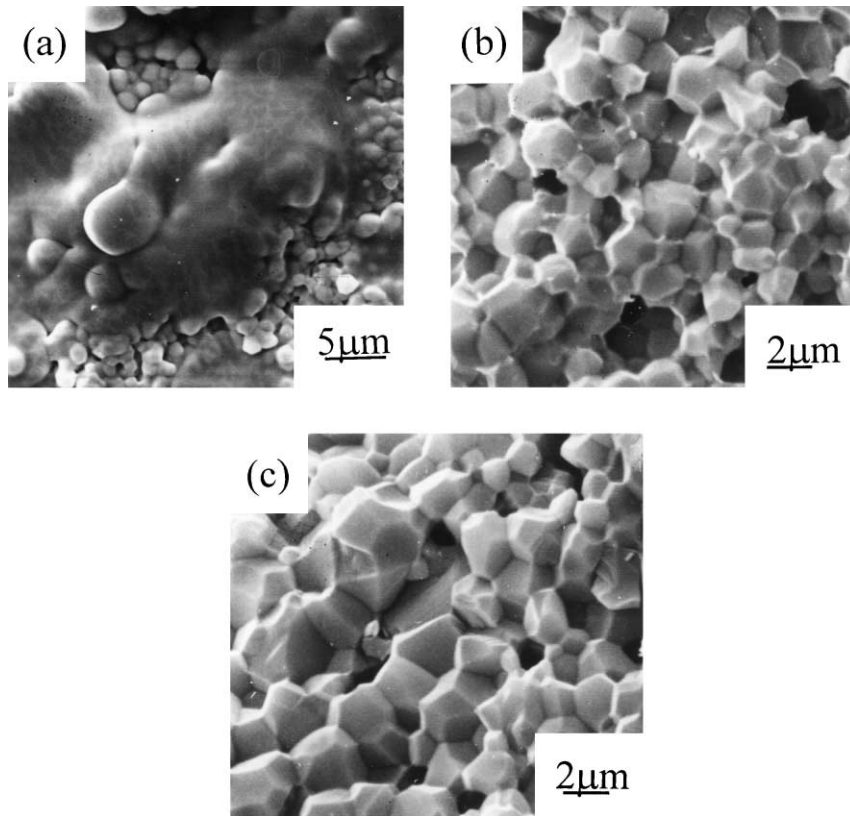


Fig. 3. Microstructures of sample CA sintered at 1650 °C for (a) 1 min, (b) 6 h, and (c) 12 h by SEM.

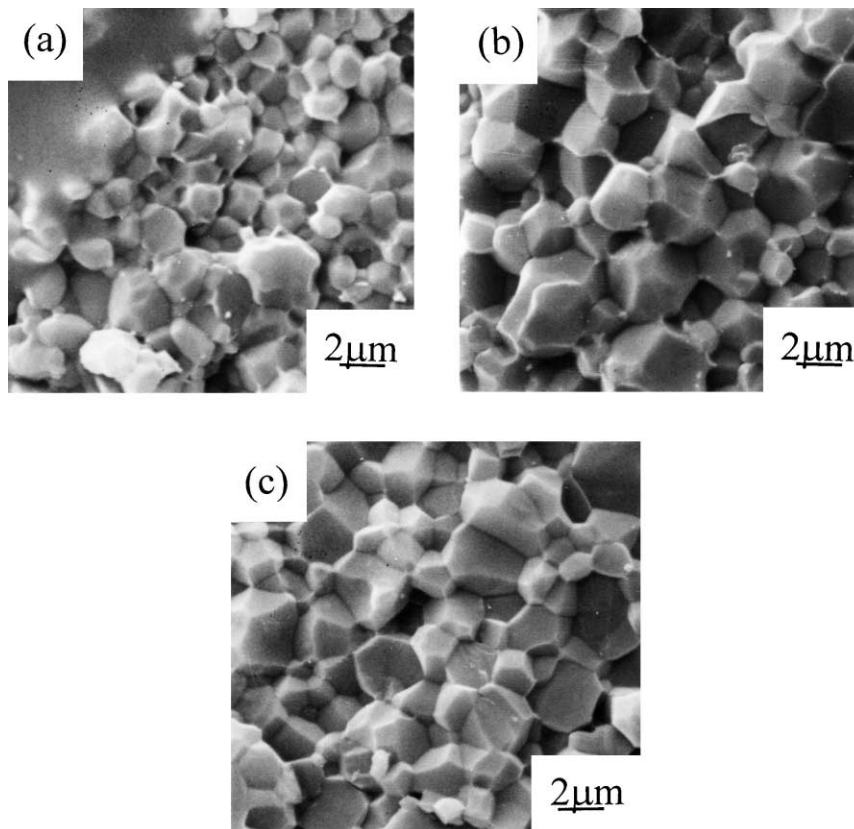


Fig. 4. Microstructures of sample CYA1 sintered at 1650 °C for (a) 1 min, (b) 6 h, and (c) 12 h by SEM.

These results are consistent with that identified by XRD, as shown in Table 3, where the two phases of YAM and  $\text{CaYAlO}_4$  are identified in this sample. By EDS as indicated in Table 4, the different contents of Ca and Y elements are examined from the edge to the middle of the grain boundary phases, which also implies the inhomogeneous phase compositions in the grain-boundary phases. It is noted that the atoms of phase YAM in field I and that of phase  $\text{CaYAlO}_4$  in field II arrange through a co-lattice transition. This implies that the promotion of the liquid  $\text{CaYAlO}_4$  on shrinkage can be reduced if the solid YAM is enough in the liquid.

### 3.4. Thermal conductivity

The qualitative information about the oxygen concentration in the AlN lattice and, indirectly, of its thermal conductivity is obtained by the careful determination of the AlN lattice parameters. A reduction of the c lattice parameter corresponds to higher oxygen concentration and lower thermal conductivity of the AlN grains.<sup>1,18,19</sup> Table 5 shows the lattice parameters, densities, and thermal conductivities of samples CA and CYA1 sintered for different time at 1650 °C. The densities of samples CA and CYA1 increase with

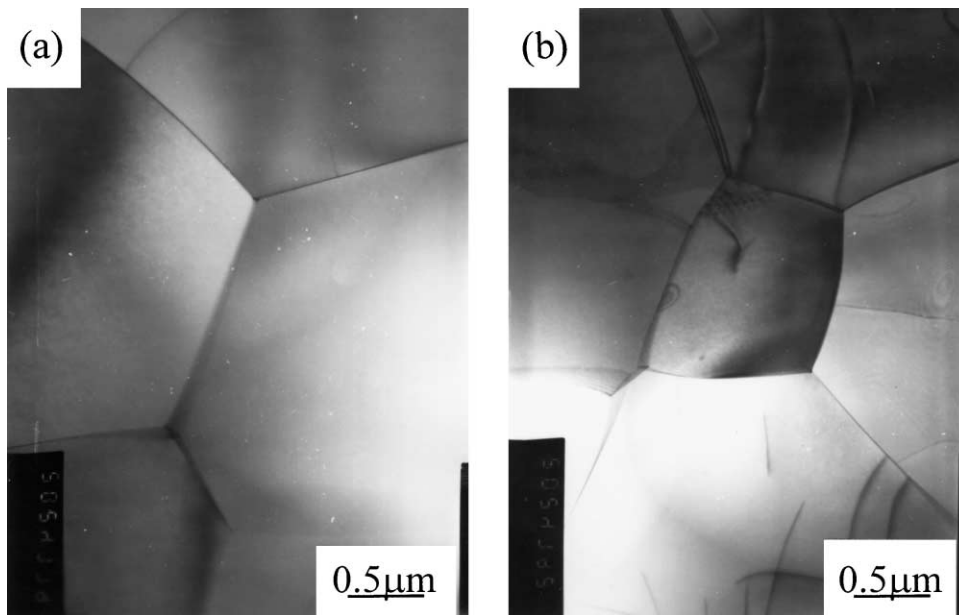


Fig. 5. TEM of samples (a) CA and (b) CYA1 sintered for 4 h at 1650 °C.

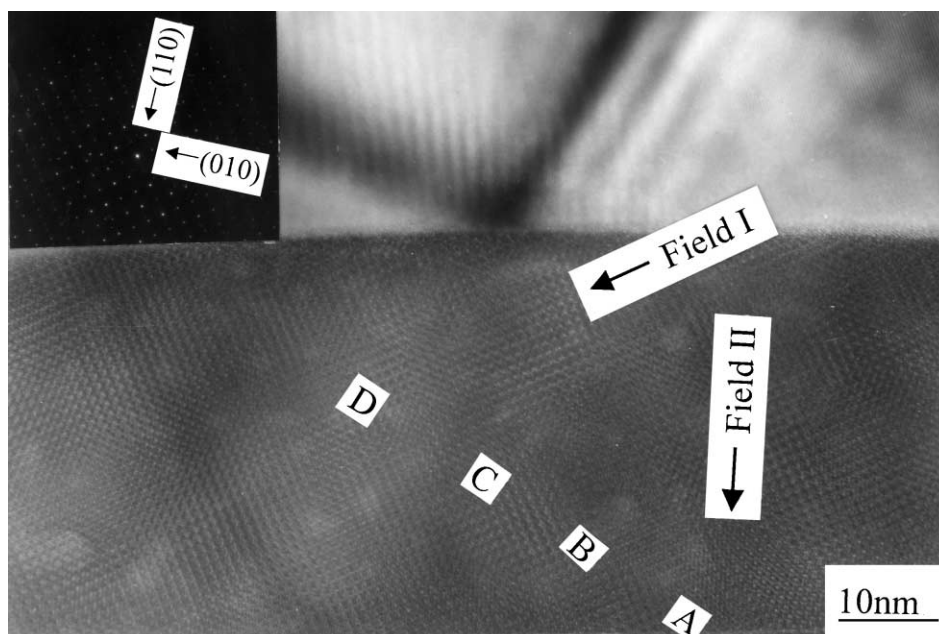


Fig. 6. High-resolution electron microscope study on the grain boundary phases of sample CYA1 sintered for 4 h at 1650 °C.

Table 4  
Contents of the elements Ca and Y in the grain boundary phases shown in Fig. 6

Position	Ca (wt.%)	Y (wt.%)	Ca/Y (atoms)
A	0.5	1.11	1
B	0.63	1.48	0.73
C	1.04	1.93	0.51
D	1.95	12.72	0.34

Table 5  
Lattice parameters, densities and thermal conductivities of samples CA and CYA1 sintered for different time at 1650 °C

Sample	a (nm)	c (nm)	Density (g/cm <sup>3</sup> )	Thermal conductivity (W/m·K)
CA for 1 min	0.31118	0.49794	2.82	85
CA for 4 h	0.31118	0.49791	3.18	121
CA for 8 h	0.31119	0.49787	3.18	120
CYA1 for 1 min	0.31119	0.49790	3.01	109
CYA1 for 4 h	0.31118	0.49789	3.24	137
CYA1 for 8 h	0.31118	0.49788	3.26	148

the sintering time, which is consistent with the shrinkages at this temperature. Since the purification of the AlN lattice produces an increase of the c-axis, the decrease of c-axis during the sintering implies that the oxygen diffuses into AlN lattice and increases the defects in it, thus deteriorating the thermal conductivity. As shown in Table 5, the c-axis in sample CA sintered from 1 min to 4 h decreases from 0.49794 to 0.49791 nm, so the increasing thermal conductivity from 85 to 121 kJ/m·K mainly comes from the enhancement of the densification. It can be seen that the density and thermal conductivity of sample CA sintered from 4 to 8 h have no change, which implies that the detriment to thermal conductivity due to the increase of the oxygen-related defects has counteracted the promotion of the decreasing grain boundary phases on it since the c-axis has a decrease from 0.49791 to 0.49787 nm. In sample CYA1 sintered from 1 min to 8 h, there is no increase on the c-axis length, which indicates that Y<sub>2</sub>O<sub>3</sub> has no prominent effect on the elimination of oxygen defects from the lattice. Furthermore, the c-axis of sample CYA1 sintered for 8 h has a very small difference from that of sample CA, which also implies that the promotion of Y<sub>2</sub>O<sub>3</sub> on the removal of oxygen from the lattice is not obvious. Thus, the higher thermal conductivity of sample CYA1 than that of CA is mainly attributed to its higher densification.

#### 4. Discussions

During the sintering, oxygen covering on the surfaces of the AlN particles diffuses into the lattice to produce aluminum vacancies, which decreases the thermal conductivity of AlN ceramics by scattering phonons. The

additives decrease the oxygen defects by two routes: (i) the additives react with the oxygen to form aluminates, and thus decrease the oxygen content on the surface of AlN particles; and (ii) the grain-boundary phases with low oxygen activity occur round the AlN grains, which removes oxygen from the lattice to the surface. To eliminate the oxygen defects in the AlN lattice, they are important that the additives contact with the AlN particles sufficiently in the route (i), and the grain-boundary phases with low oxygen activity are continuous and have the effective wetting to the AlN grains in the route (ii).

It is suggested that oxygen homogeneously distributes on the surface of the AlN particles. So it is difficult for all the oxygen to react with the additives if the liquid formed by the reaction does not wet all the AlN particles. In sample CA sintered at 1650 °C, as shown in Fig. 3, the liquid goes through a process of redistribution, which makes the oxygen on the surface of the less wetted particles by the liquid have enough time to diffuse into the lattice, thus resulting in the decrease of c-axis. Furthermore, small quantity of liquid remains between the grains, as shown in Fig. 5(a), which makes it difficult to remove the oxygen from the lattice to the surface due to the lack of the driving force produced by the liquid round the grains. So the c-axis decreases greatly and the thermal conductivity is deteriorated during the sintering. In sample CYA1, the small quantity of calcium aluminates liquid below 1650 °C not only slows the shrinkage but also decreases the close contact of Y<sub>2</sub>O<sub>3</sub> with the oxygen on the surface of the AlN particles, which results in a lower c-axis at the beginning of 1650 °C compared with that of sample CA. During the sintering, liquid CaYAlO<sub>4</sub> with Y<sub>2</sub>O<sub>3</sub> and YAM promotes the reaction between them and the oxygen, thus slowing the decrease of the c-axis. However, the effect of the liquid on the removal of the oxygen from the lattice to the surface is not prominent since the grain-boundary phases containing YAM and CaYAlO<sub>4</sub> move to the three-grain junctions as the firing time goes on, as shown in Figs. 5(b) and 6, which results in a less wetting to the AlN grains. So the c-axis of sample CYA1 decreases during the sintering. The higher thermal conductivity of the samples with Y<sub>2</sub>O<sub>3</sub> is mainly attributed to the enhancement of the densification.

#### 5. Conclusions

Y<sub>2</sub>O<sub>3</sub> has an important effect on the densification of AlN ceramics sintered at a low temperature of 1650 °C. Below this temperature, the shrinkage of the sample with Y<sub>2</sub>O<sub>3</sub> additive is slow because the solid phase reaction between Y<sub>2</sub>O<sub>3</sub> and Al<sub>2</sub>O<sub>3</sub> decreases the formation of the calcium aluminates liquid. At 1650 °C, the shrinkages of the samples with Y<sub>2</sub>O<sub>3</sub> addition increase quickly due to the formation of liquid CaYAlO<sub>4</sub>. After

sintered for 12 h, the shrinkage of the sample with 2 wt.%  $Y_2O_3$  addition reaches 17.9%, higher than that of the sample without  $Y_2O_3$  addition, which is 16.3%. In the grain-boundary phases, YAM co-exists with  $CaYAlO_4$  through a co-lattice transition, which limits the promotion of liquid  $CaYAlO_4$  on the shrinkage if the amount of YAM is too much. When the amount of  $Y_2O_3$  addition increases from 2 to 3.5 wt.%, the shrinkage of the sample decreases to 16.8%. The existence of liquid  $CaYAlO_4$  decreases the diffusion of oxygen from surface to the AlN lattice at some extent. However, the removal of the oxygen from AlN lattice is difficult because the liquid phase moves to the triple grain junction to form discrete pockets, which causes a less wetting to the AlN particles during the sintering. The increasing thermal conductivities of the samples with  $Y_2O_3$  addition mainly rely on the enhancement of the densification.

### Acknowledgements

The authors sincerely thank Professor X. Zhang and Dr. Y. Liu for the helpful discussions in this paper.

### References

- Slack, G. A., Nonmetallic crystals with high thermal conductivity. *J. Phys. Chem. Solids*, 1973, **34**, 321–335.
- Sheppard, L. M., Aluminum nitride: a versatile but challenging material. *Am. Ceram. Bull.*, 1990, **69**, 1801–1803.
- Baik, Y. and Drew, R. A. L., Aluminum nitride: processing and applications. *Key Eng. Mater.*, 1996, **122–124**, 553–570.
- Komeya, K., Inoue, H. and Tsuge, A., Role of  $Y_2O_3$  and  $SiO_2$  additions in sintering of AlN. *J. Am. Ceram. Soc.*, 1974, **54**, 411–412.
- Komeya, K., Tsuge, A. and Inoue, H., Effect of  $CaCO_3$  addition on the sintering of AlN. *J. Mater. Sci. Lett.*, 1986, **1**, 325–326.
- Huseby, I. C. and Bobik, C. F., US Patent 4 547 471, 1985.
- Virkar, A. V., Jackson, T. B. and Cutler, R. A., Thermodynamic and kinetic effects of oxygen removal on the thermal conductivity of aluminum nitride. *J. Am. Ceram. Soc.*, 1989, **72**, 2031–2042.
- Jackson, T. B., Virkar, A., More, K. L., Dinwiddie, R. B. and Cutler, R. A., High-thermal-conductivity aluminum nitride ceramics: the effect of thermodynamic, kinetic, and microstructural factors. *J. Am. Ceram. Soc.*, 1997, **80**(6), 1421–1435.
- Troczynski, T. B. and Nicholson, P. S., Effect of additives on the pressureless sintering of aluminum nitride between 1500 °C and 1800 °C. *J. Am. Ceram. Soc.*, 1989, **72**(8), 1488–1491.
- Streicher, E., Chartier, T., Boch, P., Denanot, M. F. and Rabier, J., Densification and thermal conductivity of low-sintering-temperature AlN materials. *J. Eur. Ceram. Soc.*, 1990, **6**, 23–29.
- Hashimoto, N., Yoden, H. and Deki, S., Sintering behavior of fine aluminum nitride powder synthesized from aluminum polynuclear complexes. *J. Am. Ceram. Soc.*, 1992, **75**(8), 2098–2106.
- Jarrige, J., Bouzouita, K., Doradoux, C. and Billy, M., A new method for fabrication of dense aluminium nitride bodies at a temperature as low as 1600 °C. *J. Eur. Ceram. Soc.*, 1993, **12**, 279–285.
- Liu, Y., Zhou, H., Qiao, L. and Wu, Y., Low-temperature sintering of aluminum nitride with  $YF_3$ - $CaF_2$  binary additive. *J. Mater. Sci. Lett.*, 1999, **18**, 703–704.
- Watari, K., Hwang, H. J., Toriyama, M. and Kanzaki, S., Effective sintering aids for low-temperature sintering of AlN ceramics. *J. Mater. Res.*, 1999, **14**(4), 1409–1417.
- Liu, Y., Zhou, H., Wu, Y. and Qiao, L., Improving thermal conductivity of aluminum nitride ceramics by refining microstructure. *Mater. Lett.*, 2000, **43**, 114–117.
- Greil, P., Kulig, M. and Hotza, D., Aluminum nitride ceramics with high thermal conductivity from gas-phase synthesized powders. *J. Eur. Ceram. Soc.*, 1994, **13**, 229–237.
- Wang, M. C., Hong, C. K., Tsai, M. S. and Wu, N. C., Effect of  $CaCN_2$  addition on the densification behavior and electric properties of AlN ceramics. *Jpn. J. Appl. Phys.*, 2000, **39**, 5953–5961.
- Baranda, P. S., Knudsen, A. K. and Ruh, E., Effect of CaO on the thermal conductivity of aluminum nitride. *J. Am. Ceram. Soc.*, 1993, **76**(7), 1751–1760.
- Baranda, P. S., Knudsen, A. K. and Ruh, E., Effect of yttria on the thermal conductivity of aluminum nitride. *J. Am. Ceram. Soc.*, 1994, **77**(7), 1846–1850.